J Eng Math (2020) 122:1–16
https://doi.org/10.1007/s10665-020-10041-y

The heat balance integral method for cylindrical extruders

Jacob W. Sitison · David A. Edwards

Received: 7 January 2020 / Accepted: 11 March 2020 / Published online: 13 April 2020

Abstract In the hot end of a 3-D printer, polymer feedstock flows through a heated cylinder in order to become pliable. This setup determines a natural upper limit to the speed at which the polymer may be extruded. The case of polymers which undergo the crystalline-melt transition is considered; the resulting mathematical model is a Stefan-like moving boundary-value problem for the polymer temperature. Using the heat balance integral method provides an analytical approximation for the temperature. Several different conditions which use this temperature to establish the maximum velocity are considered; using a pointwise polymer exit temperature in the hot end matches well with experimental data.

Keywords 3-D printing · Additive manufacturing · Asymptotics · Heat balance integral method · Stefan problem

1 Introduction

In recent years, the use of 3-D printing (a type of additive manufacturing) has exploded. The technique is used for everything from industrial production of prototypes to consumer production of various devices and gadgets [1]. It is often desirable to manufacture the products as quickly as possible [2,3]. However, due to the design of the printing head (as described below), there is a natural upper bound to the velocity.

In this section, we describe the experimental system only to the level of detail needed to advance our mathematical analysis. More details about parameters and the exact experimental conditions may be found in [2,3].

In a 3-D printer, a rigid polymer fiber is inserted at some pressure into a "hot end" which we consider to be a cylinder of radius R (see Fig. 1), which is typically around 1.6 mm. Within the hot end, the polymer is heated so that it becomes pliant, and then is extruded through a nozzle of smaller radius (usually an order of magnitude smaller). To reduce processing times, engineers desire to extrude the polymer as quickly as possible (velocities are on the order of mm/s). However, increasing the extrusion rate reduces the heating time, increasing the polymer's overall rigidity. This eventually leads to a case where the polymer is so rigid that the insertion pump cannot exert enough pressure to extrude it. Therefore, given a temperature differential in the hot end (which is fixed by device specifications, and is usually on the order of 100 °C), we wish to find the maximum feed velocity that will guarantee extrusion.

J. W. Sitison · D. A. Edwards (✉)
Department of Mathematical Sciences, University of Delaware, Newark, DE 19716, USA
e-mail: jsitison@udel.edu e-mail: dedwards@udel.edu

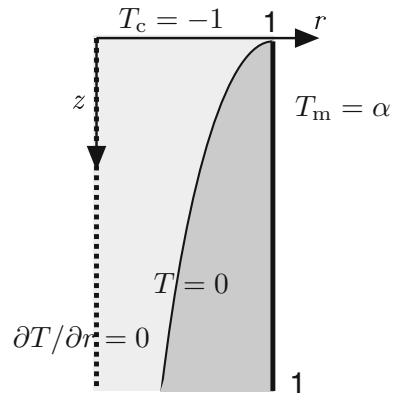

Fig. 1 Cross-section of half of hot end, dimensionless coordinates. Light area is crystalline polymer, medium area is melted polymer. The extrusion nozzle is downstream. Note we consider only up to $z = 1$

We model the system as a heat transfer problem in cylindrical coordinates in Sect. 2. For the purposes of this paper, we consider polymers such as polylactic acid (PLA), which transition from the (rigid) crystalline state to the (pliable) melted state when heated. Hence the model becomes a Stefan-like moving boundary-value problem in cylindrical coordinates.

To extend the usefulness of our results, it is important to understand the dependence of the solution upon experimental parameters. Therefore, we eschew full numerical calculations in favor of approximate analytic results. In particular, in Sect. 3 we employ the heat balance integral (HBI) method [4] for the melt state and the quasistationary approximation for the crystalline state. In Sect. 4, we discuss the dependence of the melting front on the parameters in the problem, as well as performing useful asymptotics in the limits of those parameters.

Given the mathematical solution for the temperature field, one must impose some sort of constraint on the solution which translates into a velocity bound which matches the experimental data. In Sect. 5, we consider conditions based upon average polymer temperatures: either cross-sectional at the exit or the average throughout the hot end. Neither constraint matches experimental data.

In Sect. 6, we use the exit temperature as a threshold condition. The results match the experimental data extremely well, but only in the case where we extend the melt solution beyond the interval on which it is assumed to hold. Discussions and physical interpretations of this paradox are also included in Sect. 6.

Our results demonstrate that using the exit temperature as a mathematical condition for the crystalline model produces an estimate for the velocity upper bound which matches well with experimental data. These results should help engineers to understand the dynamics of such printing mechanisms better.

2 Governing equations

We follow the work in [2] when constructing the model for the physical system, which is shown in Fig. 1. We consider heat transfer of an initially rigid crystalline polymer passing through a heater which then melts it.

Complete models for this system would be quite complex, requiring numerical approaches [5–8]. But we have a simpler, more practical goal: to calculate an upper bound on the extrusion velocity, and relate it directly to other parameters in the problem. Hence a more basic model (one which allows analytical solutions) is desirable—as long as it can fit the experimental data, which we shall demonstrate.

Therefore, in this manuscript we make several simplifying assumptions. The first group is motivated by the experimental setup and are easily justified. In particular, the problem is radially symmetric, so angular diffusion may be neglected. The aspect ratio of the heater is small [2], so diffusion in the vertical direction may be neglected. We are interested in the stationary problem, so we consider the steady-state flow after all transients have decayed away.

The second group of assumptions are implemented for mathematical simplicity:

1. The velocity is considered to be a constant V in the vertical direction. This is a realistic assumption at the inserted end because the fiber is slightly smaller than the tube, and hence will slide easily inside it. As the polymer heats, it will become more pliant: the melt state near the wall may even act as a fluid, developing into Poiseuille or more complicated non-Newtonian flow. We expect the size of these effects to be small, and in any event the *average* cross-sectional velocity must remain at V by conservation of mass. Hence we ignore the flow details in this manuscript, though they could be investigated in future research.
2. We ignore the narrowing of the hot end to the small nozzle at the extrusion point. In particular, we will solve in the portion of the hot end before it narrows, and use facts about the temperature there to determine whether the polymer will extrude.

With these assumptions, the dimensionless version of the model is given by [2]

$$\frac{\partial T}{\partial z} = \mathrm{Pe}^{-1}\frac{1}{r}\frac{\partial}{\partial r}\left(r\frac{\partial T}{\partial r}\right), \quad 0 < r < 1; \qquad \mathrm{Pe} = \frac{\rho c_p R^2 V}{kH}. \tag{1a}$$

Here Pe is the Péclet number, which contains the density ρ, the heat capacity c_p, the thermal conductivity k, the heater length H, and the cylinder radius R. The dimensionless temperature T is defined as

$$T(r,z) = \frac{\tilde{T} - T_*}{\Delta T}, \qquad \Delta T = T_* - T_\mathrm{i}, \tag{1b}$$

where $\tilde{T}$ is the dimensional temperature, T_i is room temperature, and T_* is the dimensional melting temperature. Note that with this definition $T = 0$ is the dimensionless melting temperature.

If the velocity is small, there is time for heat to diffuse through the polymer and melt it before it is extruded. Hence the engineering question is: how large can V be and still guarantee that process? In the model, small V corresponds to small Pe, where the right-hand side of (1a) dominates.

$z = 0$ corresponds to the upper end of the heater, which maintains the surface $r = 1$ at a fixed temperature $T = \alpha > 0$:

$$T_\mathrm{m}(1,z) = \alpha. \tag{2a}$$

Since $\alpha > 0$, the polymer will always be melted at the exposed surface; hence we use the subscript "m" for "melted." The crystalline polymer is inserted at room temperature, which in dimensionless variables becomes

$$T_\mathrm{c}(r,0) = -1, \tag{2b}$$

where we use the subscript "c" for "crystalline." The problem is also symmetric about the axis of the cylinder:

$$\frac{\partial T}{\partial r}(0,z) = 0. \tag{3}$$

The fact that the polymer is in both the crystalline and melt states leads to a moving boundary-value problem for the melting front $r = s(z)$ between them. The front is an isotherm at the melting temperature:

$$T_\mathrm{c}(s(z),z) = T_\mathrm{m}(s(z),z) = 0, \qquad s(0) = 1. \tag{4a}$$

The initial condition for s is determined by the boundary condition (2a), which causes immediate melting.

In addition, the standard Stefan condition states that the difference in heat flux into and out of the front is proportional to the front speed. In dimensionless coordinates, the Stefan condition for this problem becomes [2]

$$\mathrm{Pe}_\mathrm{m}^{-1}\frac{\partial T_\mathrm{m}}{\partial r}(s(z),z) - \mathrm{Pe}_\mathrm{c}^{-1}\frac{\partial T_\mathrm{c}}{\partial r}(s(z),z) = -\frac{1}{\mathrm{St}}\frac{\mathrm{d}s}{\mathrm{d}z}, \quad \mathrm{St} = \frac{\Delta T c_p}{c_\mathrm{L}}. \tag{4b}$$

Here St is the Stefan number and c_L is the latent heat of melting. In (4b), the subscripts on Pe refer to the fact that the Péclet number may be different in the two phases.

Rewriting the moving boundary-value problem completely, we obtain the following equations in the crystalline region:

$$\frac{\partial T_\mathrm{c}}{\partial z} = \frac{\mathrm{Pe}_\mathrm{c}^{-1}}{r}\frac{\partial}{\partial r}\left(r\frac{\partial T_\mathrm{c}}{\partial r}\right), \quad 0 < r < s(z); \qquad \frac{\partial T_\mathrm{c}}{\partial r}(0,z) = 0, \quad T_\mathrm{c}(r,0) = -1. \tag{5a}$$

Note that T_c holds in the rigid lightly shaded region $0 < r < s$ in Fig. 1, while T_m holds in the pliant medium shaded region $s < r < 1$, where the system becomes

$$\frac{\partial T_m}{\partial z} = \frac{\mathrm{Pe}_m^{-1}}{r}\frac{\partial}{\partial r}\left(r\frac{\partial T_m}{\partial r}\right), \quad s(z) < r < 1; \qquad T_m(1,z) = \alpha. \tag{5b}$$

As we have assumed no vertical diffusion, we cannot impose exit conditions on the heater. We thus solve the problem for all z, and then restrict our consideration of the solution for $z \in [0, 1]$, which is the dimensionless extent of the heater (see Fig. 1). In particular, the moving boundary-value problem holds only until the entire polymer is melted, at which time we would need to solve only (5b) subject to (3). However, it will be shown in the next section that the polymer never fully melts in the interval [0, 1], and so (5) is the only system we need to analyze.

By examining the behavior of the polymer while heated, we may infer what conditions are needed to make sure it is pliant enough to be extruded through the downstream nozzle. We will discuss these conditions (how to establish the temperature bound) in Sects. 5 and 6.

3 The HBI method

3.1 The crystalline region

A full solution of (5) as posed would require a full numerical simulation. However, in order to discern parameter dependence easily, it is appropriate to introduce some approximations which allow at least partial development of analytical solutions.

In the crystalline region, we employ the *quasistationary approximation*. In particular, we neglect the left-hand side of the PDE in (5a), which is equivalent to taking Pe_c (and hence V) to 0. However, by neglecting the evolution term, we will overestimate the speed of $s(z)$ [9].

Taking the left-hand side of the PDE in (5a) equal to zero leaves a second-order ODE. But there are three boundary conditions to solve in (4a) and (5a). Since we are interested in the solution throughout the interval $z \in [0, 1]$, we ignore the initial condition in (5a) to obtain the following crystalline solution:

$$T_c \equiv 0, \qquad r < s(z). \tag{6}$$

Satisfying the initial condition requires inserting a thin initial layer of width $O(\mathrm{Pe}_c)$ near $z = 0$, where there is rapid diffusion from the initial condition to (6). Therefore, as long as $\mathrm{Pe}_c \to 0$, we expect this approximation to perform well. This effect will also tend to overestimate the speed of $s(z)$, since it omits the time needed to raise the polymer to the melting temperature.

With the quasistationary approximation, the two-state Stefan problem has been reduced to a one-state Stefan problem, as (4b) is replaced by

$$\mathrm{Pe}_m^{-1}\frac{\partial T_m}{\partial r}(s(z), z) = -\frac{1}{\mathrm{St}}\frac{\mathrm{d}s}{\mathrm{d}z}. \tag{7}$$

Since our solution will use Pe only in the melt region, its value in the crystalline region is irrelevant. Using a more sophisticated approximation for the crystalline polymer is beyond the scope of this manuscript, but is discussed in Sect. 7.

3.2 The melted region

In the melted region, we approximate the solution using the HBI method. In particular, we construct a solution that does not satisfy (5b) pointwise, but averaged over the melt region $r \in [s(z), 1]$:

$$\int_{s(z)}^{1} \frac{\partial T_m}{\partial z} r\,\mathrm{d}r = \int_{s(z)}^{1} \frac{\mathrm{Pe}_m^{-1}}{r}\frac{\partial}{\partial r}\left(r\frac{\partial T_m}{\partial r}\right) r\,\mathrm{d}r.$$

Using Leibniz's Rule and (4a), we may write the above as

$$\frac{\mathrm{d}}{\mathrm{d}z}\int_{s(z)}^{1} rT_{\mathrm{m}}\,\mathrm{d}r = \int_{s(z)}^{1} \mathrm{Pe}_{\mathrm{m}}^{-1}\frac{\partial}{\partial r}\left(r\frac{\partial T_{\mathrm{m}}}{\partial r}\right)\mathrm{d}r, \tag{8}$$

which is the standard form of the HBI equation [10]. Equation (8) then replaces the equation in (5b). Despite the fact that we have now eliminated one dimension by requiring that T_{m} obey the averaged (8) instead of the pointwise (5b), the HBI method has been shown to be a quite effective approximation in the Cartesian context for the front position [4] and temperature profile [11].

The solution to the quasistationary form of (5b) is linear in $\log r$ [2], while the typical HBI approximation is quadratic [9, Sect. 3.4.C]. These considerations motivate the following form for T_{m}:

$$T_{\mathrm{m}}(r,z) = \alpha\left[a\left(1-\frac{\log r}{\log s}\right)+(1-a)\left(1-\frac{\log r}{\log s}\right)^2\right], \tag{9}$$

where a is a constant yet to be determined. Note that (9) satisfies the boundary condition in (5b) as well as the front condition (4a).

To determine a, we use an equivalent form of (7) that is more convenient for computational purposes; we follow the derivation in [11]. In particular, if we take the total derivative of (4a) with respect to z, solve for $\mathrm{d}s/\mathrm{d}z$, and substitute the result into (7), we obtain

$$\mathrm{Pe}_{\mathrm{m}}^{-1}\frac{\partial T_{\mathrm{m}}}{\partial r}(s(z),z) = \frac{1}{\mathrm{St}}\frac{\partial T_{\mathrm{m}}}{\partial z}(s(z),z)\left[\frac{\partial T_{\mathrm{m}}}{\partial r}(s(z),z)\right]^{-1}.$$

Then substituting (5b) (evaluated at $r=s$) into the above and rearranging, we have

$$\left[\frac{\partial T_{\mathrm{m}}}{\partial r}(s(z),z)\right]^2 = \frac{1}{\mathrm{St}r}\frac{\partial}{\partial r}\left(r\frac{\partial T_{\mathrm{m}}}{\partial r}\right)\Bigg|_{r=s(z)}. \tag{10}$$

Equations (10) replaces (7) as the flux front condition to be satisfied. Substituting (9) into the above and solving for a, we obtain the following:

$$a = \frac{-1+\sqrt{1+2\mathrm{St}\alpha}}{\mathrm{St}\alpha}. \tag{11}$$

It can be shown that $0 < a < 1$, so both coefficients in (9) are positive.

3.3 The cross-sectional average

For later computational purposes, it will be convenient to examine the *cross-sectional average* of T, defined as

$$\langle T\rangle(z) = 2\int_{s(z)}^{1} T_{\mathrm{m}}(r,z)r\,\mathrm{d}r, \tag{12a}$$

since $T_{\mathrm{c}}\equiv 0$. Substituting (9) into (12a), we obtain

$$\langle T\rangle(z) = \alpha\left\{1+\frac{2-a[1+s(z)^2]}{2\log s(z)}+\frac{(1-a)[1-s(z)^2]}{2[\log s(z)]^2}\right\}. \tag{12b}$$

4 The melting front

4.1 Parameter dependence

The solution is now complete with the exception of an evolution equation for s, which is provided by substituting (9) into (8):

$$\frac{\mathrm{d}s}{\mathrm{d}z} = \frac{8\mathrm{Pe}_{\mathrm{m}}^{-1}(1-a)s(\log s)^2}{2-2a+(2-a)\log s+s^2[2a(\log s)^2+(2-3a)\log s-2(1-a)]}. \tag{13}$$

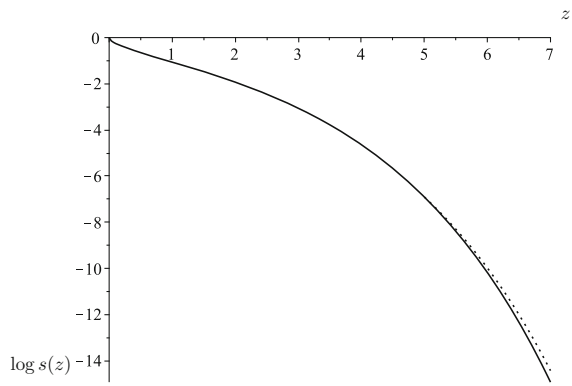

Fig. 2 Graphs of the solutions to (13) (solid curve) and (14) with $z_0 = 5$ (dotted curve)

We may use (13) to verify our previous claim that the polymer never completely melts (which corresponds to $s = 0$) while it is being heated. Expanding (13) for small s, we obtain

$$\frac{\mathrm{d}s}{\mathrm{d}z} \sim \frac{8\mathrm{Pe}_\mathrm{m}^{-1}(1-a)s\log s}{2-a},$$

the solution of which is given by

$$s(z) \sim \exp\left(\log s_0 \exp\left(\frac{8\mathrm{Pe}_\mathrm{m}^{-1}(1-a)(z-z_0)}{2-a}\right)\right), \tag{14}$$

where $s(z_0) = s_0$ would be set by the matching conditions. As predicted, $s(z) > 0$ for any finite z. From a physical perspective, this is a shortcoming of the model, since we expect that the entire polymer will melt in finite time. However, for the purposes of fitting experimental data, the more important consideration is what conditions we impose on the solution, as will be discussed in Sects. 5 and 6.

To demonstrate the accuracy of the asymptotic approximation, we first select some parameter values. We use

$$\mathrm{St} = 2.52, \tag{15a}$$

as given in [2], as well as

$$\alpha = \mathrm{St}^{-1}, \qquad \mathrm{Pe}_\mathrm{m} = 4.5903, \tag{15b}$$

which are values consistent with experimental data (see next section). The rather odd value of α may be explained by noting that $s(z)$ depends on neither α or St separately, but rather on their product through the definition of a in (11). It can be shown that $\mathrm{St}\alpha$ is independent of ΔT [2], which is consistent with the one-phase approximation, which effectively assumes that the polymer enters the chamber at $T = 0$.

We demonstrate the accuracy of the asymptotic approximation in Fig. 2. The solid curve shows the solution to (13) with the parameters in (15); the dotted curve shows a graph of (14), where $z_0 = 5$ and s_0 is chosen to match the solid curve. Note the good agreement for larger z. Moreover, since $0 < a < 1$ and $\log s_0 < 0$, $s(z) = 0$ only in the limit that $z \to \infty$. Therefore, we never have to consider the case where the entire cross section of the polymer is melted. Thus the appropriate evolution equation is given by (5b) for all $z \in [0, 1]$: the heated region of interest.

In Figs. 3 and 4, we show the dependence of $s(z)$ on parameters in the problem. In particular, in Fig. 3 we show that increasing α increases the progression of $s(z)$. This is consistent with the physical interpretation, since larger α means a larger temperature differential, which will generate more melting.

In Fig. 4, we show that increasing Pe_m slows the progression of $s(z)$. This is consistent with the physical interpretation, since larger Pe_m corresponds to a higher polymer velocity. Hence the polymer is exposed to the heater for a shorter period of time, inhibiting melting.

To illustrate the temperature profiles, we plot (9) for various values of z in Fig. 5 for the same parameters as in (15). To the left of the graph for each z, the polymer is crystalline with $T_\mathrm{c} = 0$. The derivative is discontinuous at that point; it is this discontinuity that drives the motion of $s(z)$ via (7). As z gets larger, the temperature becomes

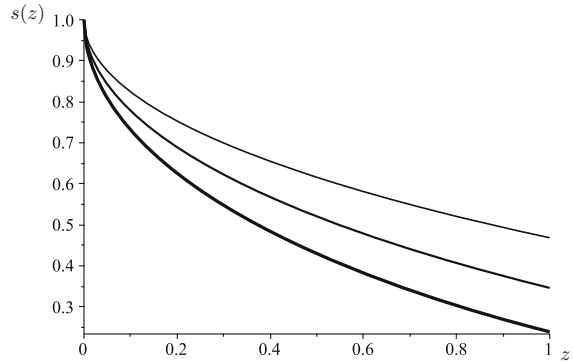

Fig. 3 $s(z)$ vs. z for (in increasing order of thickness) $\alpha = (2\mathrm{St})^{-1}$, St^{-1}, $2\mathrm{St}^{-1}$

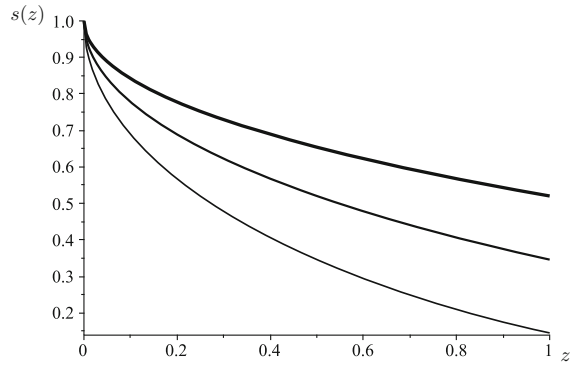

Fig. 4 $s(z)$ vs. z for (in increasing order of thickness) $\mathrm{Pe_m}$ half as big, the same size, and twice as big as the value in (15b)

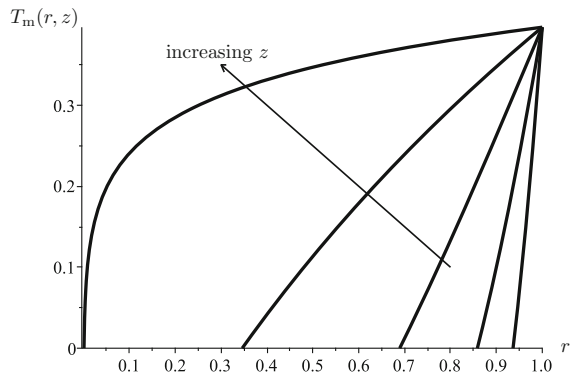

Fig. 5 Graphs of (9) for $z = 0.008$, 0.04, 0.2, 1, and 5. For each z, the temperature is 0 to the left of the r-intercept

more concave down, and a smaller region remains crystallized, becoming vanishingly small when $z = 5$. Note that for the parameters shown, the polymer remains 1/3 crystalline when it exits the heater ($z = 1$).

4.2 Asymptotics

For later purposes, it is convenient to examine the behavior of s, T, and $\langle T\rangle(z)$ in the asymptotic limits of small and large $\mathrm{Pe_m}$.

Small $\mathrm{Pe_m}$ corresponds to infinitesimally slow flow, which gives the entire polymer time to melt. For small $\mathrm{Pe_m}$, the right-hand side of (13) becomes large, which corresponds to quick decay of $s(z)$ to 0 [which can also be seen directly from (14)]. Substituting this result into (12b) yields

$$\langle T\rangle(z) \sim \alpha, \qquad \mathrm{Pe_m} \to 0. \tag{16}$$

Large $\mathrm{Pe_m}$ corresponds to very fast flow. As the polymer is then exposed to the heater for only a short amount of time, we expect $s(z)$ to remain near 1. In particular, substituting $s(z) \sim 1 - \mathrm{Pe_m}^{-m} f(z)$ into (13), we obtain, to leading order,

$$-\mathrm{Pe_m}^{-m}\frac{\mathrm{d}f}{\mathrm{d}z} \sim \frac{8(1-a)\mathrm{Pe_m}^{-(1+2m)} f^2}{-2(2+a)\mathrm{Pe_m}^{-3m} f^3/3}, \qquad f(0) = 0, \tag{17}$$

from which we have that $m = 1/2$ and

$$s(z) \sim 1 - \mathrm{Pe_m}^{-1/2} f(z), \quad f(z) = 2\sqrt{\frac{6(1-a)z}{2+a}}, \qquad \mathrm{Pe_m} \to \infty. \tag{18}$$

To obtain (12b) in this limit, we first note from (18) that the region of integration $1 - s(z)$ in (12a) is $O(\mathrm{Pe_m}^{-1/2})$, and $T_\mathrm{m} = O(1)$, so $\langle T\rangle(z) = O(\mathrm{Pe_m}^{-1/2})$. We note from (12b) that $\langle T\rangle$ can also be considered as a function of s; hence we may use a Taylor series and the order-of-magnitude result to obtain the following:

$$\langle T\rangle(z) \sim \beta \mathrm{Pe_m}^{-1/2} f(z), \quad \mathrm{Pe_m} \to \infty; \qquad \beta = \left|\frac{\mathrm{d}\langle T\rangle}{\mathrm{d}s}(1)\right|. \tag{19a}$$

A laborious calculation provides the value

$$\beta = \frac{\alpha(a+2)}{3}. \tag{19b}$$

It will also be convenient to examine the behavior of s in the asymptotic limit of small α, which corresponds to heating just above the melting point. Hence we expect the melting front to remain close to the heater, and we substitute $s(z) \sim 1 - \alpha^n g(z)$ into (13) to obtain, to leading order,

$$-\alpha^n \frac{\mathrm{d}g}{\mathrm{d}z} = \frac{8\mathrm{Pe_m}^{-1}(1-a)\alpha^{2n} g^2}{-2(2+a)\alpha^{3n} g^3/3}, \qquad g(0) = 0, \tag{20}$$

which is similar in structure to (17). Then using the fact that

$$a \sim 1 - \frac{\mathrm{St}\alpha}{2}, \quad \alpha \to 0, \tag{21}$$

we find that the dominant balance has $n = 1/2$ and

$$s(z) \sim 1 - \alpha^{1/2} g(z), \quad g(z) = 2\sqrt{\frac{\mathrm{St}z}{\mathrm{Pe_m}}}, \qquad \alpha \to 0. \tag{22}$$

Note that (22) is exactly the small-α limit of (18).

5 Temperature averages as flow constraints

The solution as described in the previous section provides only one piece of information needed to fit experimental data. The second piece is a condition on the temperature that corresponds to a state that allows extrusion of the polymer. In this section, we consider two conditions which depend on temperature averages. These types of conditions have proved successful with amorphous polymers [2].

5.1 Cross-sectional average at exit

As the polymer is hottest at the exit of the cylindrical heater ($z = 1$), it is natural to impose a constraint there which will determine whether the polymer will extrude. In particular, we require that the cross-sectional average of the temperature at the exit $\langle T\rangle(1)$ must exceed some threshold value T_t. This condition can also be motivated by viscosity considerations [2].

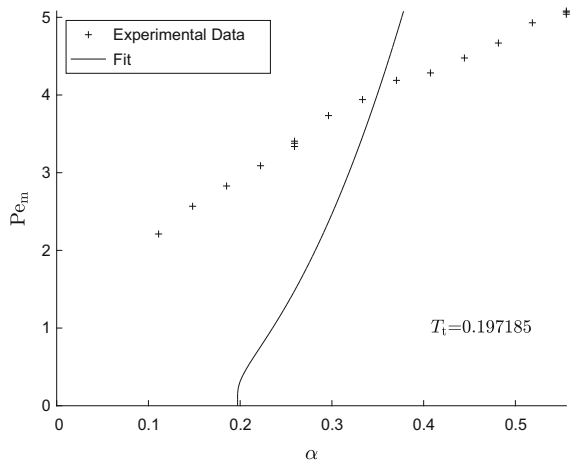

Fig. 6 Graph of (23) and experimental data

Substituting $z = 1$ into (12b), this condition becomes

$$T_t = \alpha\left\{1 + \frac{2 - a[1 + s(1)^2]}{2\log s(1)} + \frac{(1-a)[1 - s(1)^2]}{2[\log s(1)]^2}\right\}, \tag{23}$$

where we have taken equality as the constraining case. The expression (23) is then fit (using Matlab) to experimental data from [3] given the value of St in (15a). Unless otherwise noted, the data fit is for a 0.35 mm extrusion nozzle diameter. The parameters needed to transform the dimensional experimental data into $(\alpha, \mathrm{Pe_m})$ coordinates may be found in [2].

Since the only fit parameter is T_t, its value may be determined by just computing the average of the right-hand side of (23), evaluated at each of the data points. The computation of the right-hand side of (23) is complicated by the unusual behavior of (13) near $s = 0$. In particular, if the parameters are such that $s(z)$ is very small in the region of interest, it can happen that the Matlab integrator can "overshoot" $s = 0$, producing imaginary values. To handle this situation, for small enough s we replace the numerical integration of (13) with the asymptotic solution (14), which has already been demonstrated as effective.

The results are shown in Fig. 6, which are clearly unusable for predictive purposes. Here the fit curve is shown as a solid curve; the extrusion region corresponds to any values of $(\alpha, \mathrm{Pe_m})$ under it.

The graph does illustrate some interesting facets of the solution. First, as predicted by (16), as $\mathrm{Pe_m} \to 0$, the cross-sectional average tends to α, so the α-intercept of the curve is T_t. Second, as $\mathrm{Pe_m} \to \infty$, we may replace the right-hand side of (23) with (19) evaluated at $z = 1$, yielding

$$T_t = \beta \mathrm{Pe_m}^{-1/2} f(1) \qquad \Longrightarrow \qquad \mathrm{Pe_m} = \left[\frac{(a+2)f(1)}{3T_t}\right]^2 \alpha^2, \quad \mathrm{Pe_m} \to \infty. \tag{24}$$

$\mathrm{Pe_m} \to \infty$ corresponds to $\alpha \to \infty$, which from (11) corresponds to $a = 0$. Hence the curve approaches a quadratic which is concave up. Physically, we note that as $\mathrm{Pe_m} \to \infty$, the feed speed becomes infinitely large. Therefore, in order to maintain an average temperature above the threshold, the temperature must become infinitely large as well, which corresponds to $\alpha \to \infty$.

Last, the fit looks particularly bad to the eye, even given the nature of the fit curve. However, recall that the curve fitting is not the standard version of minimizing $|\mathrm{Pe_m} - \mathrm{Pe_{fit}}(\alpha)|^2$. Instead, we are minimizing $|T_t - \langle T\rangle(1; \mathrm{Pe_m}, \alpha)|^2$. In other words, we are finding the contour line of $\langle T\rangle(1; \mathrm{Pe_m}, \alpha)$ which is closest to those running through each of the experimental data points.

The polymer will be hottest near the heater at $r = 1$. Consequently, in this region the polymer will have the lowest viscosity and the highest propensity to "flow." Therefore, one might consider a more useful average to take would be one just in this heated region; for example, a thin layer of size δ. In that case, (12a) would be replaced by

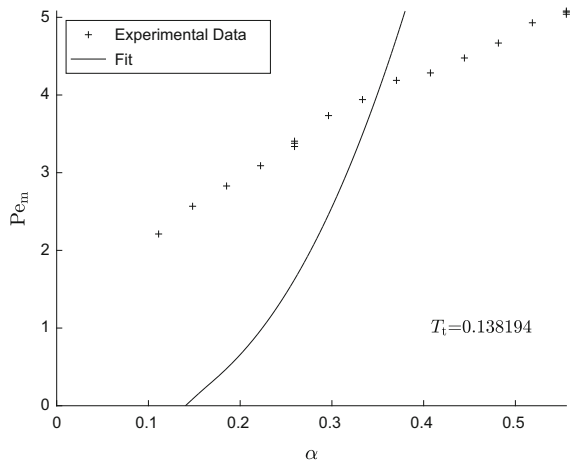

Fig. 7 Graph of (26b) and experimental data

$$\langle T\rangle(z) = \frac{2}{\delta(2-\delta)}\int_{\delta}^{1} T_{\mathrm{m}}(r,z)r\,\mathrm{d}r. \tag{25}$$

However, a study of that case leads to similarly poor results as in Fig. 6, for reasons similar to those described above.

5.2 Full average in cylinder

With the cross-sectional average providing such a poor fit, we are forced to consider other conditions. It has been shown [2] that the pressure head needed to force the polymer through the extruder is dependent on the average viscosity *in the entire cylinder*. In that work, the authors use the average *temperature* in the cylinder as a stand-in for the average viscosity and obtain good results in the amorphous case (which has no change of state). We define $\bar{T}(z)$ to be the *cumulative cross-sectional temperature* up to the length z; hence it follows the evolution equation

$$\frac{\mathrm{d}\bar{T}}{\mathrm{d}z} = \langle T\rangle(z), \qquad \bar{T}(0) = 0, \tag{26a}$$

where again we have used the fact that the temperature in the crystalline region is zero. Since the cylinder is of normalized length 1, the average temperature in the cylinder is $\bar{T}(1)$.

Equating this with the threshold temperature and using (12b), the constraining condition becomes

$$T_{\mathrm{t}} = \bar{T}(1) = \alpha + \alpha\int_0^1 \frac{2-a[1+s(z)^2]}{2\log s(z)} + \frac{(1-a)[1-s(z)^2]}{2[\log s(z)]^2}\,\mathrm{d}z. \tag{26b}$$

Equation (26b) is in a convenient form for comparison with (23). However, for numerical purposes the form (26a) is more convenient, as s and $\bar{T}$ can be integrated simultaneously, reducing computational time.

The expression (26b) is then fit (using Matlab) to experimental data as before. Again, the only fit parameter is T_{t}, and we use (14) as necessary to obtain appropriate values for s.

The results are shown in Fig. 7, which are still unusable for similar reasons to those discussed before. The fit curve has a similar shape: as $\mathrm{Pe_m} \to 0$, the average of (16) is still α, so the α-intercept of this fit curve is also T_{t}. Similarly, as $\mathrm{Pe_m} \to \infty$, we may substitute (19a) into (26b), which simply yields (24) with $f(1)$ replaced by the average of f in z, which is still positive. Hence the average curve fit also approaches a quadratic which is concave up, and the physical interpretation is the same as before. The fit is bad for similar reasons to those discussed above.

Lastly, note that the fully averaged fit has a lower value of T_{t} than the cross-sectional fit. Physically, since the polymer is continually heated for $z \in [0, 1]$, the cross-sectional average at $z = 1$ will be the hottest in the polymer, so $\bar{T}(1) < \langle T\rangle(1)$. Hence to achieve extrusion with the same data points, the threshold T_{t} needs to be less in the fully averaged case, as shown in the graph.

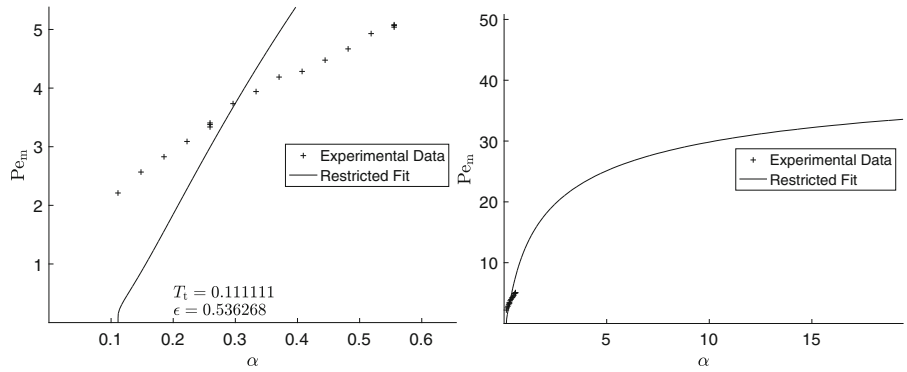

Fig. 8 Left: Graph of (27b) (forced to have $T_t \geq 0$) and experimental data. Right: Graph showing asymptotic behavior

6 Exit temperature as threshold condition

The poor agreement in Figs. 6 and 7 motivates a reconsideration of the threshold condition. The material properties of the crystalline state make it significantly more difficult to extrude than the melted state. Hence for extrusion we would like to eliminate the proportion of crystalline polymer at the end of the cylinder.

Mathematically, this is not possible, since as discussed in Sect. 4, our model does not allow complete melting of the cross section for any finite z. Hence we postulate the following condition:

$$T_t = T_m(\epsilon, 1; \mathrm{Pe}_m, \alpha), \qquad \epsilon > 0. \tag{27a}$$

Note that in this case, there are now two fit parameters: ϵ and T_t. Motivated by our work in the previous sections, the best fit is established using Matlab by minimizing $|T_t - T_m(\epsilon, 1; \mathrm{Pe}_m, \alpha)|^2$. Substituting (9) into (27a), we obtain

$$T_t = \alpha\Big[ay + (1-a)y^2\Big], \quad y = 1 - \frac{\log \epsilon}{\log s(1)}. \tag{27b}$$

6.1 Results

Under our model, the crystalline solution is exactly zero; therefore, from theoretical considerations it seems appropriate to restrict the threshold temperature $T_t \geq 0$, which would then force $\epsilon \geq s(1)$ for any experiment.

The results are shown in Fig. 8. As discussed in Sect. 4.2, $s(1) \to 0$ as $\mathrm{Pe}_m \to 0$, so the right-hand side of (27b) tends to α, so the α-intercept of the curve is T_t. Here it is more convenient to look at large-α asymptotics. Expanding (11) for large α, we find that $a = O(\alpha^{-1/2})$. Substituting this result into (27b) yields a quadratic on the right-hand side in $\alpha^{1/2}y$. This must balance the $O(1)$ value of T_t, so $y = O(\alpha^{-1/2})$, which from (27b) implies that

$$s(1) = \epsilon(1 + \alpha^{-1/2}s_1), \qquad \alpha \to \infty, \tag{28}$$

where s_1 is a negative constant.

We note from (18) that if $\mathrm{Pe}_m \to \infty$ as $\alpha \to \infty$, this would force $\epsilon = 1$, which forces the right-hand side of (27b) to 0 for all parameter values. Hence $s(1)$ must remain bounded away from 1, which implies that Pe_m asymptotes to a constant as $\alpha \to \infty$. This in turn implies that the fit curve must be concave down, as shown at the right of Fig. 8.

This behavior may also be explained by noting that as discussed above, $a \to 0$ as $\alpha \to \infty$, so the leading order of (13) is independent of α in that limit. Hence as $\alpha \to \infty$, $s(1)$ will asymptote to a constant. Physically, at high enough temperature, the front position is set by the velocity only (through Pe_m), as shown at the graph at right of Fig. 8.

In addition to the poor experimental fit in Fig. 8, the code also experiences some anomalies. In particular, given different starting positions, the code will iterate to different fit parameters. This indicates that there may be several

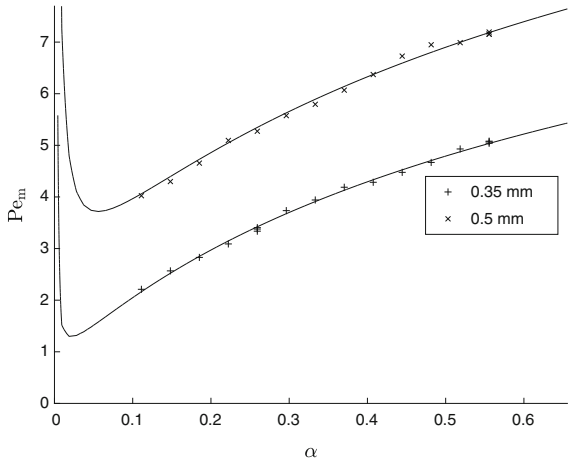

Fig. 9 Graph of (27b) (T_t unrestricted) and experimental data

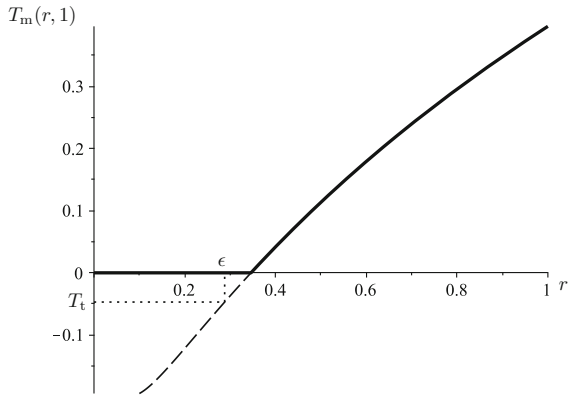

Fig. 10 Graph of (9) for $z = 1$. Solid curve: Modeled solution. Dashed curve: extension of melt solution into crystalline region

local minima in the problem. Moreover, one of the returned fit sets has $T_t = 0$, which indicates that the true global minimum may occur for negative T_t.

Therefore, we take the unorthodox step of relaxing the code's restriction on the sign of T_t, which then allows ϵ to be less than $s(1)$, and y to be negative.

The results are shown in Fig. 9. The fit is astonishingly good, not only for the 0.35-mm data we have been using for comparison, but also for another data set with an extrusion diameter of 0.5 mm. With the restriction removed, the code consistently returns the same negative value of T_t, so we have found the global minimum. In particular, for the 0.35-mm case, we have

$$T_t = -0.030711, \qquad \epsilon = 0.28791.$$

Allowing T_t to be negative greatly improves the fit, but how can it be justified? Consider Fig. 10, which illustrates the temperature profile at $z = 1$ for the parameters in the Appendix. The solid curve shows the temperature as modeled: namely with $T_c \equiv 0$. The dashed curve shows the extension of the melt temperature into the crystalline region.

Thus from a computational perspective, the code is just imposing the threshold condition in the crystalline region, where the temperature is just an extension of the melt temperature. Given the good fit with experimental data, this motivates the belief that in the neighborhood of the melting front, the true temperature in the crystalline must be well-approximated by the extension of the melt temperature. (Note this correspondence does not extend to the profile itself, as there must be a discontinuity in the derivative at the melting front to drive its evolution.)

As discussed above, as $\mathrm{Pe_m} \to 0$ the right-hand side of (27b) tends to $\alpha > 0$, while the left-hand side is now negative. Hence there is no solution to the equality in this limit, as shown in Fig. 9. Instead, there is a minimum in the fit curve. Physically, this means that for a slow enough velocity, flow will occur at any imposed temperature. That is because the temperature threshold the polymer has to surpass is now negative, while $\alpha > 0$.

Substituting (21) into the right-hand side of (27b) and expanding for small α yields a quadratic in αy. Hence $y = O(\alpha^{-1})$, which means that $s(1)$ must be near 1. Substituting (22) into (27b), we have

$$y \sim \frac{\log \epsilon}{\alpha^{1/2} g(1)} \propto -\sqrt{\frac{\mathrm{Pe_m}}{\alpha}}.$$

Therefore, the only way that $y = O(\alpha^{-1})$ is if $\mathrm{Pe_m} \propto \alpha^{-1}$, as shown at left in Fig. 11. In other words, for small temperatures, $s(1)$ has to be incredibly close to 1 for the inequality to fail. This occurs only when $\alpha \to 0$ *and*

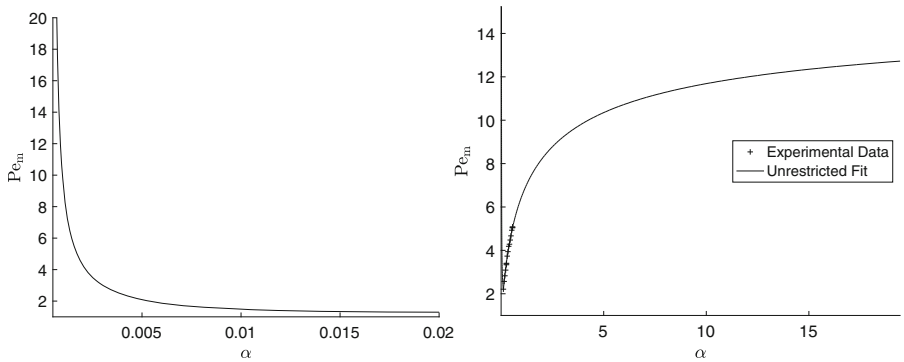

Fig. 11 Left: Graph of fit for small α. Right: Graph of fit for large α

$\mathrm{Pe_m} \to \infty$: just one of those two limits is not enough. Alternatively, as $\alpha \to 0$, the melt profile shown in Fig. 10 becomes nearly horizontal, so its extension remains very close to 0, which means that it will exceed moderate negative values of T_t.

The asymptotics for large α proceed as in the case where $T_\mathrm{t} \geq 0$; the constant asymptote is shown at right in Fig. 11.

7 Conclusions and further research

Engineers who wish to optimize production using a 3-D printing process desire to know the maximum rate at which the polymer construction material can be extruded. The polymer feedstock is heated as it moves through the hot end, which increases its pliability. Since increasing the velocity reduces the heating time, an upper bound on the velocity exists. Beyond that point, the polymer has not been heated for long enough for it to be pliable enough to be extruded.

Given several physically realistic simplifying assumptions, we modeled the system by the heat equation in cylindrical coordinates. We considered the case of polymers which undergo the crystal-melt transition; hence the underlying system is a Stefan-like moving boundary-value problem, where the moving boundary is the melting front $s(z)$.

We solved the system using a quasistationary approximation in the crystal and the HBI method in the melt. This reduced the system to the temperature field described by (9) and (11), coupled to the ODE (13) for the melting front. This ODE had to be solved numerically, with an analytic approximation (14) used when the problem became too stiff.

As expected, the front speed increased with increasing α, as the heater temperature is increased. Similarly, the front speed increased with decreasing $\mathrm{Pe_m}$, as the flow velocity is decreased, allowing more time for the polymer to heat.

Given a solution for the temperature field, it is then incumbent upon us to formulate a condition that translates the solution into an upper bound for the velocity. We examined three possibilities. Following the analysis for the amorphous case in [2], we first considered imposing a constraint on the cross-sectional exit temperature. However, as shown in Fig. 6, the fit was poor and had the wrong concavity for large values of $\mathrm{Pe_m}$. The fact that the overall shape of the curve did not fit the data leads us to conclude that introducing additional degrees of freedom (either by adding parameters or allowing T_t to be negative, as in Sect. 6) would not appreciably improve the fit.

Similarly, a constraint using the average temperature in the entire cylinder, though found to match amorphous polymer data well in [2], also failed to fit the PLA data (see Fig. 7). In an amorphous polymer, the pliancy increases gradually, and so it makes sense that the polymer would need to have an average temperature over some threshold in order to extrude. In contrast, a polymer like PLA has two separate states. Thus, it is natural to track how much

of the polymer is in the crystalline state upon extrusion. If the crystalline core is too large, we would expect that to prevent extrusion.

With this motivation, we imposed the exit temperature condition (27a). From a mathematical perspective we would expect the threshold temperature T_t to be positive, since the temperature in the crystalline state was modeled to be exactly zero. But fitting the data with such a constraint on T_t was unsuccessful, and by monitoring the internal progress of the computational fit, we could see that the true best fit occurred for $T_t < 0$.

When we removed the constraint on T_t, the fit to data was astonishingly good, as shown in Fig. 9. Thus the model works well...in the region where experiments are actually performed. However, due to the negative threshold temperature, unusual results appeared in the limits of small α and $\mathrm{Pe_m}$. In particular, we would expect on physical grounds that the curve would have an α-intercept, as shown in the other figures.

So how to reconcile these positive and negative traits? The answer is shown in Fig. 10. Essentially, by allowing a negative T_t, we are extending the melt solution outside its region of validity. In the experimental cases of moderate α and $\mathrm{Pe_m}$, the extension closely matches the solution profile, and the curve fits the data. Outside those regimes, the extension does not match the solution profile, leading to spurious results.

One obvious solution is to replace the quasistationary approximation in the crystalline regime with the more refined HBI method. Unfortunately, the use of the HBI method in a problem like ours is quite tricky. Authors tend to avoid cylindrical coordinates [12], or use a semi-discretized approach [13]. One problem is that a solution of the form (9), which would be the best form for matching behavior at the front $s(t)$, becomes singular at $r = 0$. Using a standard Taylor series causes difficulty in matching the front evolution behavior. However, an exponential approach (as in [14]) may show promise due to the use of a similarity-type variable.

Nevertheless, the improvement of the model in the crystalline region, perhaps using a Megerlin approach [9, §3.4], is a subject of further research. Other areas of future research are full numerical simulations to verify our HBI results, and refining our results by relaxing the assumptions in Sect. 2.

In conclusion, our results show that using the exit temperature threshold condition (27a) provides strong predictive behavior of the velocity upper bound in experimentally important regimes. In particular, given a desired velocity, our solution predicts the temperature differential required, even when beyond the range of commercially available equipment. However, as shown in Fig. 11, increasing the temperature provides diminishing returns in increasing the velocity bound. This agrees with our physical intuition, since it takes time for heat to diffuse through the polymer, and so the bound will be unreachable at high speeds. Such insight should be able to assist engineers in designing better and more productive 3-D printers.

Nomenclature

Variables and parameters

Units are listed in terms of length (L), mass (M), time (T), and temperature (θ). If a symbol appears both with and without tildes, the symbol with tildes has units, while the one without is dimensionless. Equation numbers where a variable first appears is listed, if appropriate.

- a: Dimensionless constant (9).
- c_L: Latent heat of melting, units L^2/T^2 (4b).
- c_p: Heat capacity of polymer, units $L^2/(T^2\theta)$ (1a).
- H: Length of heater, units L (1a).
- k: Thermal conductivity, units $ML/(T^3\theta)$ (1a).
- m: Scaling exponent (17).
- n: Scaling exponent (20).
- Pe: Péclet number (1a).
- R: Radius of cylinder, units L (1a).
- r: Radial coordinate (1a).

St: Stefan number (4b).
$s(z)$: Front between states, units L (4a).
$\tilde{T}(r, z)$: Temperature, units θ (1).
V: Velocity in z-direction, units L/T (1a).
y: Variable used in pointwise condition (27b).
z: Distance along the channel, units L (1a).
α: Dimensionless temperature at heater (2a).
β: Coefficient in cross-sectional average calculation (19a).
ΔT: Differential between transition and room temperature, units θ (1b).
δ: Dimensionless width of layer near heated surface (25).
ϵ: Radius used in pointwise condition (27a).
ρ: Density of polymer, units M/L^3 (1a).

Other notation

c: as a subscript on T, used to indicate temperature in the crystalline region (2b).
i: as a subscript on T, used to indicate room temperature (1b).
m: as a subscript on T, used to indicate temperature in the melted region (2a).
t: as a subscript on T, used to indicate the extrusion transition (23).
*: as a subscript on T, used to indicate the melting temperature (1b).
$\langle\cdot\rangle$: used to indicate a cross-sectional average (12a).
$\bar{}$: used to indicate an average over the whole device (26a).

Acknowledgements The authors thank the Office of Undergraduate Research and Experiential Learning at the University of Delaware for their support of this project. We also thank the reviewers for their insightful comments which helped improve this manuscript. Many of the calculations herein were performed with the assistance of Maple and Matlab.

References

1. Gibson I, Rosen DW, Stucker B (2009) Additive manufacturing technologies: rapid prototyping to direct digital manufacturing, 1st edn. Springer Publishing Company, Incorporated, New York, NY
2. Edwards DA, Mackay ME, Swain ZR, Banbury CR, Phan DD (2019) Maximal 3D printing extrusion rates. IMA J Appl Math 84(5):1022–1043
3. Mackay ME, Swain ZR, Banbury CR, Phan DD, Edwards DA (2017) The performance of the hot end in a plasticating 3D printer. J Rheol 61(2):229–236
4. Wood AS (2001) A new look at the heat balance integral method. Appl Math Model 25(10):815–824
5. Lotero F, Couenne F, Maschke B, Sbarbaro D (2017) Distributed parameter bi-zone model with moving interface of an extrusion process and experimental validation. Math Comput Modell Dyn Syst 23(5):504–522
6. Mu Y, Zhao G, Wu X, Hang L, Chu H (2015) Continuous modeling and simulation of flow-swell-crystallization behaviors of viscoelastic polymer melts in the hollow profile extrusion process. Appl Math Model 39(3–4):1352–1368
7. Sandoval Murillo JL, Ganzenmueller GC (2017) A convergence analysis of the affine particle-in-cell method and its application in the simulation of extrusion processes. In: Wriggers P, Bischoff M, Onate E, Owen D, Zohdi T (eds) V International conference on particle-based methods-fundamentals and applications (Particles 2017). European Community on Computatational Methods in Applied Sciences, International Association for Computational Mechanics, Barcelona, pp 397–408
8. Schoinochoritis B, Chantzis D, Salonitis K (2017) Simulation of metallic powder bed additive manufacturing processes with the finite element method: a critical review. Proc Inst Mech Eng B 231(1):96–117
9. Alexiades V, Solomon AD (1992) Mathematical modeling of melting and freezing processes. Taylor & Francis, Washington
10. Goodman TR (1961) The heat-balance integral-further considerations and refinements. J Heat Transf 83(1):83–85
11. Mitchell SL, Myers TG (2010) Application of standard and refined heat balance integral methods to one-dimensional stefan problems. SIAM Rev 52(1):57–86
12. Ren HS (2007) Application of the heat-balance integral to an inverse Stefan problem. Int J Thermal Sci 46(2):118–127

13. Caldwell J, Chin C (1998) Solution of two-phase Stefan problems by the heat balance integral method. In: Tupholme GE, Wood AS (eds) Institute of mathematics and its applications conference series. Oxford University Press, Oxford, pp 131–137
14. Mosally F, Wood A, Al-Fhaid A (2002) An exponential heat balance integral method. Appl Math Comput 130(1):87–100